

# Implications of the dark axion portal for the muon $g - 2$ and $B$ -factories

Patrick deNiverville,<sup>1</sup> Hye-Sung Lee,<sup>2</sup> and Min-Seok Seo<sup>3</sup>

<sup>1</sup>*Center for Theoretical Physics of the Universe, IBS, Daejeon 34126, Korea*

<sup>2</sup>*Department of Physics, KAIST, Daejeon 34141, Korea*

<sup>3</sup>*Department of Physics, Chung-Ang University, Seoul 06974, Korea*

(Dated: June 2018)

The dark axion portal is a recently introduced portal between the standard model and the dark sector. It connects both the dark photon and the axion (or axion-like particle) to the photon simultaneously through an anomaly triangle. While the vector portal and the axion portal have been popular venues to search for the dark photon and axion, respectively, the new portal provides new detection channels if they coexist. The dark axion portal is not a result of the simple combination of the two portals, and its value is not determined by the other portal values; it should be tested independently. In this paper, we discuss implications of the new portal for the leptonic  $g - 2$  and  $B$ -factories. We provide the model-independent constraints on the axion-photon-dark photon coupling and discuss the sensitivities of the recently activated Belle-II experiment, which will play an important role in testing the new portal.

## I. INTRODUCTION

Our universe can be divided into two sectors: the visible and the dark. The visible sector of the universe is comprised of the standard model (SM) particles, whose constituents were all identified with the last discovery of the Higgs boson in 2012 [1, 2]. Just as the SM has various kinds of fermions, gauge bosons, and a scalar boson, the dark sector might also have a rich spectrum of dark fermions, dark gauge bosons, and dark scalar bosons rather than a single dark matter (DM) particle. Although there has been no discovery of the dark sector particles so far, the existence of the dark sector is backed by significant observational evidence of DM [3].

It is natural to expect that there is a connection between the SM particles and DM particles other than gravity as the typical explanations (freeze-out, freeze-in [4]) of the dark matter relic density require an interaction between the two sectors. While it is possible the dark sector particles carry the SM weak charges (as in many supersymmetric dark matter models), it may also be very possible they do not carry any charges under the SM gauge symmetries. Even in the latter case, two separate sectors might still be able to communicate with each other if there is a ‘portal,’ a way to connect the visible sector particles and the dark sector particles through a mixing or a loop-effect.

There have been four popular portals:

- (i) Vector portal:  $\frac{\epsilon}{2\cos\theta_W} B_{\mu\nu} Z'^{\mu\nu}$ ,
- (ii) Axion portal:  $\frac{G_{a\gamma\gamma}}{4} a F_{\mu\nu} \tilde{F}^{\mu\nu}, \dots$ ,
- (iii) Higgs portal:  $\kappa |S|^2 H^\dagger H, \dots$ ,
- (iv) Neutrino portal:  $y_N L H N$ .

The constraints on these portals can be found in Refs. [3, 5, 6]. The relic DM can be either a portal particle or a particle coupled to portal particles via hidden interactions (for examples see Refs. [7, 8]).

The vector portal [9] is a mixing between a SM gauge boson and a dark sector gauge boson (such as dark photon [7] and the dark  $Z$  [10], which is a variant of the dark

photon with an axial coupling [11–17]). The axion portal connects the axion or axion-like particle to a pair of the SM gauge bosons. Recently, it was pointed out that a ‘dark axion portal’ [18]) may exist, connecting the dark photon and axion to the SM. The new portal is independent from the vector and axion portals as it arises from a different mechanism.

When a new portal is introduced, it can provide new opportunities to search for dark sector particles [5]. For some of the recent studies using the dark axion portal, see Refs. [19–23]. Because of the very small couplings between the dark sector and the SM particles, their masses can be much smaller than the typical (electroweak - TeV) scale of new physics. As a matter of fact, most of the studies of the portal focus on the rather light masses as we can see in the dark photon and axion (or axion-like particle) cases. (For some mechanisms to introduce very light particles, see Refs. [24–26].) Various studies can be summarized in a similar fashion as in Ref. [27] that show the constraints on the vast parameter space of the portal particle (mass and coupling).

In this paper, we study the implications of the dark axion portal for a roughly MeV - 10 GeV scale dark photon, the mass range focused on by the typical intensity frontier new physics [5]. We investigate possible signals of the new portal at the  $B$ -factories and use the existing data from the BaBar experiment to constrain the axion-photon-dark photon coupling. We also study the sensitivities of the new Belle-II experiment for both Phase II and Phase III running. Belle-II began data taking in April 2018 with a partially complete detector, and will be one of the major players in the intensity frontier physics over the next decade. We also study the implications for the muon and electron  $g-2$  and determine the constraints on the new coupling from existing measurements.

While we focus on MeV - 10 GeV scale physics, much heavier particles can be searched for by energy frontier experiments such as the LHC experiments; much lighter ones may be observed by the cosmic frontier observations such as stellar cooling and supernovae.

The exact nature of the axion-photon-dark photon coupling is model dependent and the predictions may change depending on other related couplings (such as the axion-photon-photon and axion-dark photon-dark photon couplings), but we will treat it in a model-independent way by taking the limit where only axion-photon-dark photon coupling is relevant.

In Sec. II, we briefly discuss the dark axion portal vertex, and elaborate on our parameterization. In Sec. III, we discuss the search channels and constraints for the dark axion portal from the BaBar and Belle-II experiments. In Sec. IV, we discuss the contributions to the electron and muon  $g - 2$  from the new axion-photon-dark photon vertex and obtain constraints from current measurements. In Sec. V, we provide a summary of our study and future directions.

## II. DARK AXION PORTAL

The axion portal and the dark axion portal terms [18] can be written as following.

$$\begin{aligned}\mathcal{L}_{\text{axion portal}} &= \frac{G_{agg}}{4} a G_{\mu\nu} \tilde{G}^{\mu\nu} + \frac{G_{a\gamma\gamma}}{4} a F_{\mu\nu} \tilde{F}^{\mu\nu} + \dots \quad (1) \\ \mathcal{L}_{\text{dark axion portal}} &= \frac{G_{a\gamma'\gamma'}}{4} a Z'_{\mu\nu} \tilde{Z}'^{\mu\nu} + \frac{G_{a\gamma\gamma'}}{2} a F_{\mu\nu} \tilde{Z}'^{\mu\nu} \quad (2)\end{aligned}$$

The dark axion and the axion portal are constructed using the anomaly triangle and the actual couplings depend on the details of the model. For instance, in the dark KSVZ axion model introduced in Ref. [18], the portal couplings are given as

$$G_{a\gamma\gamma} = \frac{e^2}{8\pi^2} \frac{PQ_\Phi}{f_a} \left[ 2N_C Q_\psi^2 - \frac{2}{3} \frac{4+z}{1+z} \right], \quad (3)$$

$$G_{a\gamma'\gamma'} \simeq \frac{ee'}{8\pi^2} \frac{PQ_\Phi}{f_a} [2N_C D_\psi Q_\psi] + \varepsilon G_{a\gamma\gamma}, \quad (4)$$

$$G_{a\gamma'\gamma'} \simeq \frac{e'^2}{8\pi^2} \frac{PQ_\Phi}{f_a} [2N_C D_\psi^2] + 2\varepsilon G_{a\gamma\gamma}, \quad (5)$$

where  $N_C = 3$  is the color factor.  $e$  ( $e'$ ) and  $Q_\psi$  ( $D_\psi$ ) are the electric (dark) coupling constant and charge of the exotic quarks in the anomaly triangle.  $f_a/PQ_\Phi$  is the mass scale of the exotic quarks.  $z = m_u/m_d \simeq 0.56$  is the mass ratio of the  $u$  and  $d$  quarks.  $\varepsilon$  is the vector portal coupling which we take to be 0 in our study.

While one can consider the coupling in the context of a specific model that can decide the couplings in terms of the model parameters and provide connections among them, we focus on the limit where a model independent treatment makes sense and consider only the  $G_{a\gamma\gamma'}$  coupling. Specifically, we take  $m_a \ll m_{\gamma'}$  and also take the view the model-specific part of the  $G_{a\gamma\gamma}$  such as the electric charge contribution are arranged to make  $G_{a\gamma\gamma}$  small enough to neglect its effect in the analysis we perform in this paper.

We do not claim that the  $a$  should be the QCD axion, but take it to an axion-like particle with a mass much

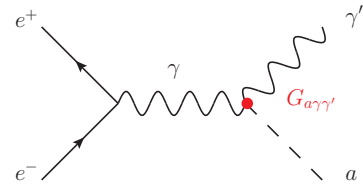


FIG. 1. Electron-positron annihilation to on-shell  $a$  and  $\gamma'$ . Observable at  $B$  factories as a monophoton produced through subsequent decay  $\gamma' \rightarrow \gamma a$ .

smaller than that of the  $\gamma'$ . The  $G_{a\gamma'\gamma'}$  is nonzero, but the on-shell decay process  $a \rightarrow \gamma'\gamma'$  is kinematically forbidden, while the off-shell process would be negligibly small. While the decay  $a \rightarrow \gamma\gamma$  is allowed, by considering a very small  $m_a$ , the aforementioned arrangement to minimize  $G_{a\gamma\gamma}$  would ensure the  $a$  is sufficiently long-lived to escape the  $B$ -factory detectors before its decay and its effect on the lepton  $g - 2$  is suppressed, making the effect of the  $G_{a\gamma\gamma}$  negligible in our analysis. More general cases and their implications will be studied in subsequent works.

## III. LIMITS FROM B FACTORIES

### A. BaBar

BaBar [28] is an asymmetric electron-positron collider with a 9 GeV electron beam and a 3.1 GeV positron beam for a center of mass energy of 10.5 GeV. The experiment collected an integrated luminosity of over  $500 \text{ fb}^{-1}$  [29] between 1999 and 2008, but the monophoton trigger was only implemented for its final running period.

We examine the process  $e^+e^- \rightarrow a\gamma'$  shown in Fig. 1, and calculated with FeynCalc [30, 31] to be

$$\frac{d\sigma}{dt} = \frac{\alpha_{\text{EM}} G_{a\gamma\gamma'}^2}{16s^3} (2m_{\gamma'}^4 - 2m_{\gamma'}^2(s+t+u) + t^2 + u^2), \quad (6)$$

where  $s = (p_{e^-} + p_{e^+})^2$ ,  $t = (p_{\gamma'} - p_{e^-})^2$  and  $u = (p_a - p_{e^-})^2$  are the Mandelstam variables. This process can result in the production of a monophoton final state through a subsequent  $\gamma' \rightarrow a\gamma$  decay, so long as the  $\gamma'$  is reasonably prompt. We will assume that  $m_a \ll m_{\gamma'}$ ,

	Low-Cut	High-Cut
$E_\gamma^*$	[2.2, 3.7] GeV	[3.2, 5.5] GeV
$\cos\theta_\gamma^*$	[-0.46, 0.46]	[-0.31, 0.6]
Luminosity	$19 \text{ fb}^{-1}$	$28 \text{ fb}^{-1}$
Efficiency	55%	30%

TABLE I. Kinematic cuts on the BaBar Low-Cut and High-Cut samples.  $E_\gamma^*$  is the center of mass energy of the detected photon and  $\theta_\gamma^*$  is the angle of the photon relative to the beam axis in the center of mass frame.

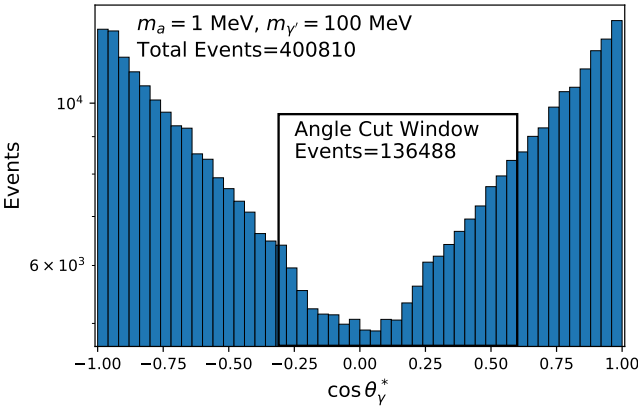


FIG. 2. As an illustration, we provide a histogram of the cosine of the center-of-mass emission angle  $\cos \theta_\gamma^*$  for a sample of  $4 \times 10^6$  secondary decay photons produced through  $e^+e^- \rightarrow a(\gamma' \rightarrow a\gamma)$  for High-Cut energies. The boxed window reflects the imposed High-Cut  $\cos \theta_\gamma^*$  range detailed in Table I. Of the  $10^6$  events initially generated,  $1.36 \times 10^5$  survive both the energy and angle cuts. The bin size for this histogram was chosen to provide a good representation of the angular distribution, but is not relevant to the analysis.

and that the  $a$  is sufficiently long-lived to escape the BaBar detector before decaying radiatively. We follow the approach of Ref. [32] in using BaBar’s  $\Upsilon(3S) \rightarrow \gamma A0$  data, where  $A0$  is some invisibly decaying scalar particle [33]<sup>1</sup>. This set of data records the measured center-of-mass energy of detected monophotons,  $E_\gamma^*$ . The data is divided into overlapping Low-Cut and High-Cut  $E_\gamma^*$  domains, where the Low-Cut domain is  $E_\gamma^* \in [2.2, 3.7] \text{ GeV}$ , and the High-Cut domain is  $E_\gamma^* \in [3.2, 5.5] \text{ GeV}$ . See Table I for a summary of the cuts, luminosities and efficiencies.

Samples of  $10^6$   $e^+e^- \rightarrow a\gamma'$  events were generated with CalcHEP 3.6.27 [35, 36] for 45 dark photon masses. The subsequent  $\gamma' \rightarrow a\gamma$  decays were simulated using an external Python code. As in Ref. [32], the simulated photons were smeared using a Crystal Ball function (see Ref. [37]) with  $n = 1.79$ ,  $\alpha = 0.811$  and  $\sigma/(E_\gamma^*) = 0.015 \times (\text{GeV}/E_\gamma^*)^{3/4} + 0.01$ . In the absence of a background model, we will place a conservative limit on the coupling constant  $G_{a\gamma\gamma'}$  by treating all measured events as signal, and taking the maximum value of  $G_{a\gamma\gamma'}$  for which the theory prediction does not exceed the measured number of events in any bin of either the High- or Low-Cut data by more than  $2\sigma$ .

A sample of the angular distribution of photons produced in the chain  $e^+e^- \rightarrow a(\gamma' \rightarrow a\gamma)$  is shown in Fig. 2. The events from  $e^+e^- \rightarrow a\gamma(\gamma' \rightarrow a\gamma)$  could be poten-

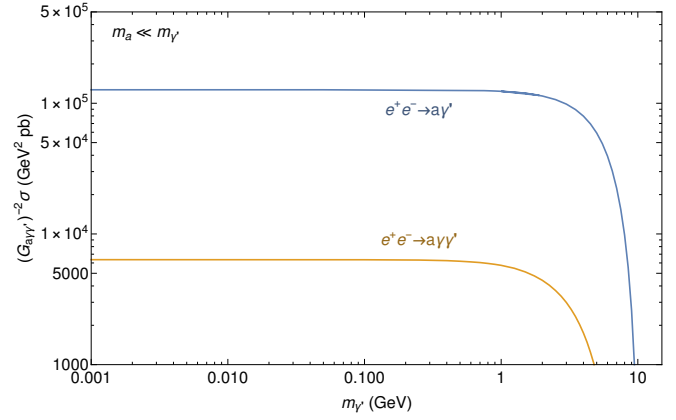


FIG. 3. Cross sections for the processes  $e^+e^- \rightarrow a\gamma'$  and  $e^+e^- \rightarrow a\gamma\gamma'$  with  $m_a \ll m_{\gamma'}$ .  $E_\gamma \in [2.2, 5.5] \text{ GeV}$ . The cross section of  $e^+e^- \rightarrow a\gamma\gamma'$  is heavily suppressed relative to  $e^+e^- \rightarrow a\gamma'$  due in part to the three body final state.

tially relevant, as the primary photon is preferentially emitted along the beam axis while the secondary photon produced through the  $\gamma'$  decay has a much broader angular distribution and frequently passes the required monophoton cuts. However, this process possesses a much smaller cross section than pure annihilation (compare the lines shown in Fig. 3) and would contribute at a subleading level to the observed monophoton signal.

We show the limits obtained by BaBar, using only  $e^+e^- \rightarrow a(\gamma' \rightarrow a\gamma)$ , for  $m_a \ll m_{\gamma'}$  in Fig. 4. For  $m_{\gamma'} \leq 100 \text{ MeV}$ , the lifetime can become sufficiently large for relevant values of  $G_{a\gamma\gamma'}$  that dark photons begin to escape the detector before they decay, reducing the number of observed monophoton events:

$$c\tau_{\gamma'} \approx \frac{5.95 \times 10^{-14} \text{ m} \cdot \text{GeV}}{G_{a\gamma\gamma'}^2 m_{\gamma'}^3} \quad (\text{for } m_a \ll m_{\gamma'}) \quad (7)$$

$$\approx 60 \text{ m} \times \left( \frac{10^{-3} \text{ GeV}^{-1}}{G_{a\gamma\gamma'}} \right)^2 \times \left( \frac{1 \text{ MeV}}{m_{\gamma'}} \right)^3. \quad (8)$$

This is reflected in a pronounced shoulder in the limit contour as, due to the decline in  $m_{\gamma'}$ , the lifetime of the  $\gamma'$  becomes  $\mathcal{O}(1 \text{ m})$ , a length comparable in size to the BaBar detector.

## B. Belle-II

The Belle-II experiment [39] is the successor to the Belle and BaBar experiments, and has recently begun taking data as part of Phase II of its operations. Phase II aims to record  $20 \text{ fb}^{-1}$  of integrated luminosity with a partially completed detector, while Phase III of the experiment will take  $50 \text{ ab}^{-1}$  of data with the completed detector and the SuperKEKB particle accelerator. Unlike BaBar, Belle-II will run with a monophoton trigger for the entirety of its run. To estimate the sensitivity of Belle-II to the  $a\gamma\gamma'$  vertex, samples of  $10^6 e^+e^- \rightarrow \gamma\gamma'a$

<sup>1</sup> The limits we will place using this data could potentially be improved by using a larger BaBar analysis that included a background model [34].

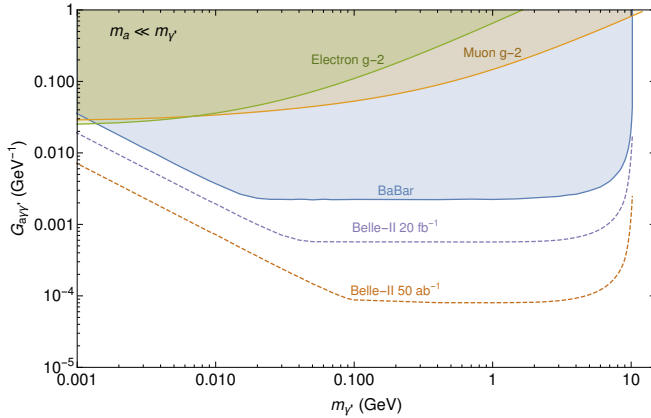


FIG. 4. Limits placed on  $G_{a\gamma\gamma'}$  for the hierarchical mass scenario with  $m_a \ll m_{\gamma'}$  by a BaBar monophoton search and measurements of lepton  $g - 2$ . Also shown are projected sensitivities for Phase-II and III of the Belle-II experiment.

events were generated with CalcHEP 3.6.27 [35, 36] for 48 values of  $m_{\gamma'}$  chosen so as to smoothly render all features of the contour. Photons were generated through the decay of the  $\gamma'$  and the number satisfying the preliminary cuts shown in Ref. [40] were recorded. This preliminary analysis predicted that 300 background events would survive these cuts for  $20 \text{ fb}^{-1}$  of data, and we scale this to  $7.5 \times 10^5$  background events for  $50 \text{ ab}^{-1}$ .

We show contours for the expected Phase-II and Phase-III luminosities, with  $2\sqrt{300}$  events for the  $20 \text{ fb}^{-1}$  contour, and  $2\sqrt{7.5} \times 10^5$  events for the  $50 \text{ ab}^{-1}$  contour for  $m_a \ll m_{\gamma'}$  in Fig. 4. Thanks to a combination of greater luminosity and generous angular cuts, Belle-II is capable of probing far smaller values of  $G_{a\gamma\gamma'}$  than BaBar.

#### IV. CONSTRAINTS FROM LEPTON $g - 2$

The dark axion model introduces the new two-loop contribution to the lepton anomalous magnetic moment shown in Fig. 5. The change to lepton  $a_\ell = (g - 2)/2$  is given by [41, 42]:

$$\Delta a_\ell = \frac{\alpha}{\pi} \int_0^1 dx (1-x) \Pi_R(s_x) - \frac{\alpha}{3\pi} c m_\ell^2 G_{a\gamma\gamma'}^2, \quad (9)$$

where  $c$  is a positive free parameter introduced during the renormalization of the  $a\text{-}\gamma\text{-}\gamma'$  vertex (see App. A for further details),

$$s_x \equiv -\frac{x^2}{1-x} m_\ell^2, \quad (10)$$

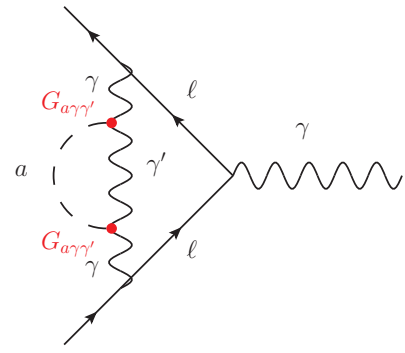


FIG. 5. Two-loop diagram providing the leading contribution to lepton anomalous magnetic moment including  $a\text{-}\gamma\text{-}\gamma'$  vertices.

and

$$\Pi_R(q^2) = \Pi(q^2) - \Pi(0) - q^2 \Pi'(0) \quad (11)$$

$$= \int_0^1 dx \left[ \log \left( \frac{xm_a^2 + (1-x)m_{\gamma'}^2}{xm_a^2 + (1-x)m_{\gamma'}^2 - x(1-x)q^2} \right) \right. \\ \left. \times (xm_a^2 + (1-x)m_{\gamma'}^2 - x(1-x)q^2) - \frac{q^2}{6} \right]. \quad (12)$$

While the free parameter  $c$  makes the theory unpredictable, both terms that contribute to  $\Delta a$  are always negative, and conservative limits can be placed on  $G_{a\gamma\gamma'}$  by assuming  $c = 0$ , as non-zero values of  $c$  will only magnify the effect of the dark axion portal contribution and correspondingly improve the limits. The current best measurements of the anomalous magnetic moment of the muon come from a muon storage ring at Brookhaven National Laboratory [43–46]. Their measurement exceeds the theoretically predicted value by  $3.5\sigma$  [3],

$$\Delta a_\mu = a_\mu(\text{exp}) - a_\mu(\text{SM}) = (26.8 \pm 7.6) \times 10^{-10}. \quad (13)$$

The dark axion portal unfortunately exacerbates this disagreement. We place a limit where the SM+dark axion portal increases  $\Delta a_\mu$  by  $15.2 \times 10^{-10}$ , a  $5.5\sigma$  disagreement. In the future, the E989 collaboration at Fermilab intends to improve on the precision of the current experimental measurement by a factor of three [47].

The electron anomalous magnetic moment has been determined most accurately through one-electron quantum cyclotron experiments and measurements of the ratio between the Planck constant and the mass of Rubidium-87 [48–50]. The theory prediction [51] exceeds experimental measurements by approximately  $1\sigma$  [52],

$$\Delta a_e = a_e(\text{exp}) - a_e(\text{SM}) = -(1.06 \pm 0.82) \times 10^{-12}. \quad (14)$$

The dark axion portal can reduce the disagreement between theory and experiment of the electron anomalous magnetic moment. We place a limit where the dark axion portal contribution overcorrects the difference between the SM and experiment, and  $a_e$  disagrees with the experimentally measured value by more than  $2\sigma$ . Both this

contour and that derived for muon  $g - 2$  are shown in Fig. 4.

While the two-loop contribution from the dark axion portal cannot resolve the muon  $g - 2$  discrepancy (because of the wrong sign), the situation could become nontrivial if we allow for the model-dependent contributions from  $a$ -fermion-fermion Yukawa couplings or  $a$ - $\gamma$ - $\gamma$  coupling ( $G_{a\gamma\gamma'}$ ). As studied in Ref. [53], the combined effect of Bar-Zee one-loop diagrams and light-by-light and vacuum polarization two-loop diagrams might resolve the muon  $g - 2$  discrepancy if sufficiently large coupling strengths are allowed. We will study this more general situation in subsequent works.

## V. SUMMARY AND DISCUSSION

We studied implications of the dark axion portal for the lepton  $g - 2$  and  $B$ -factories in the  $m_a \ll m_{\gamma'}$  limit. We focused on the dark photon masses for which  $B$ -factories provide the greatest sensitivity, roughly from 1 MeV to 10 GeV, and we restricted our plotted results to this window in Fig. 4. BaBar and Belle-II have too little energy to produce an on-shell  $\gamma'$  with a mass much larger 10.2 GeV. It is important to consider the lifetime of the  $\gamma'$  for  $m_{\gamma'}$  below a hundred MeV, as it becomes increasingly likely that the dark photon will escape the detector before decaying in an observable fashion. The mass reach could be extended in both directions by considering off-shell dark photon production through the process  $e^+e^- \rightarrow a\gamma'^* \rightarrow a a\gamma$ , though this cross section is suppressed by several orders of magnitude relative to  $e^+e^- \rightarrow a\gamma'$ . We also investigated the effects on both the muon and electron  $g - 2$  in a conservative manner, though they only imposed meaningful constraints at relatively low masses.

While we have restricted our attention to monophoton searches at asymmetric  $B$ -factories,  $e^+e^-$  colliders could potentially probe the scenario in other ways. As mentioned in Ref. [53] in the context of axion-like particles,  $e^+e^- \rightarrow e^+e^- + a\gamma'$  is an intriguing channel, with final states ranging from  $e^+e^- +$  missing energy to  $e^+e^- +$  multiple photons depending on the lifetimes of the dark particles, but has yet to see an experimental analysis.

Evidence of  $\gamma \rightarrow a\gamma'$  conversion may also be found in radiative meson decays, but the rapid decay of the  $\gamma'$  complicates the signal for larger values of  $m_{\gamma'}$ . For long-lived  $\gamma'$ 's, we can compare the limit of  $\text{Br}(\pi^0 \rightarrow \gamma\nu\bar{\nu}) < 6 \times 10^{-4}$  placed by Ref. [54] to the branching fraction of  $\pi^0 \rightarrow a\gamma\gamma'$ , a decay with a similar end-state. Unfortunately, this branching fraction is quite small, and the possible limit of  $G_{a\gamma\gamma'} \gtrsim 1 \text{ GeV}^{-1}$  is not competitive with those placed by electron or muon  $g - 2$ . For a short-lived  $\gamma'$ , the signal would be  $\pi^0 \rightarrow \gamma\gamma + \text{Missing Energy}$ , which would require a measurement of the invariant mass distribution of the end-state photons. Limits could also be derived by comparing  $K^+ \rightarrow \pi^+\nu\bar{\nu}$  [55] to  $K^+ \rightarrow$

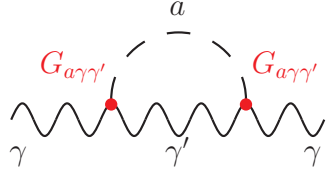


FIG. 6. New photon vacuum polarization diagram that contributes to  $\Pi^{\mu\nu}(q^2)$  with the introduction of the  $a$ - $\gamma$ - $\gamma'$  vertex.

$\pi^+(\gamma \rightarrow a\gamma')$  or  $\phi \rightarrow \pi^0\gamma$  to  $\phi \rightarrow \pi^0a(\gamma' \rightarrow a\gamma)$  [56]. For much larger masses, one could look to the Higgs decay  $H \rightarrow \gamma\gamma^* \rightarrow \gamma\gamma + \text{Missing Energy}$ .

Future directions of interest involve exploring the implications of a long-lived  $\gamma'$  more thoroughly, as past beam dump experiments such as CHARM or E137 (see Ref. [5] for a thorough overview) and planned experiments such as SHiP [57] could be sensitive to monophotons produced through  $\gamma' \rightarrow a\gamma$ . In the case of very long-lived dark photons, inelastic  $a$  or  $\gamma'$  scattering inside the detectors of beam dump experiments, fixed target neutrino experiments [58–60], or for few MeV masses, reactor neutrino experiments [61, 62] could also be useful search avenues. Missing momentum/energy experiments such as NA64 [63] provide another probe of the parameter space that may be worth consideration. For masses below 1 MeV, constraints from stellar cooling and supernovae become interesting, as both the  $a$  and the  $\gamma'$  provide potential vectors for additional energy loss [64], as well as production from the sun [65].

## ACKNOWLEDGMENTS

This work was supported in part by IBS (Project Code IBS-R018-D1), NRF Strategic Research Program (NRF-2017R1E1A1A01072736), NRF Basic Science Research Program (NRF-2016R1A2B4008759) and CAU Research Grants in 2018. HL appreciates hospitality of the Pitt-PACC at University of Pittsburgh during the Light Dark World International Forum 2017.

## Appendix A: Renormalization and Lepton $g - 2$

As mentioned in Sec. IV, the dark axion portal introduces a new two-loop contribution (see Fig. 5) to the lepton  $g - 2$ . This contribution is not renormalizable, and we will require additional counter terms to eliminate the new divergences. The first step is to calculate the sub-diagram in Fig. 6, the dark axion portal contribution to

the photon vacuum polarization,

$$i\Pi^{\mu\nu} = -\frac{1}{F^2} \int \frac{d^4}{(2\pi)^4} \frac{\epsilon^{\sigma\mu\rho\delta}\epsilon_\sigma^{\nu\beta\gamma}k_\rho q_\delta k_\beta q_\gamma}{[k^2 - m_{\gamma'}^2][(k+q)^2 - m_a^2]} \quad (\text{A1})$$

$$\equiv i\Pi(q^2)(q^2 g^{\mu\nu} - q^\mu q^\nu)$$

where

$$\Pi(q^2) = \frac{G_{a\gamma\gamma'}^2}{(4\pi)^2} \int_0^1 dx [xm_a^2 + (1-x)m_{\gamma'}^2 - x(1-x)q^2] \left( \frac{2}{\epsilon} - \gamma + \log(4\pi) - \log(xm_a^2 + (1-x)m_{\gamma'}^2 - x(1-x)q^2) \right). \quad (\text{A2})$$

The integral in Eq. (A2) is quadratically divergent, and we will need to add an additional quadratically divergent term to the lagrangian to cancel the infinities,

$$\mathcal{L}_{\text{dark axion portal}} \ni \frac{c}{4\Lambda^2} \partial_\rho F_{\mu\nu} \partial^\rho F^{\mu\nu}, \quad (\text{A3})$$

where  $c$  is a free parameter, and  $\Lambda$  is some cut-off scale. The most straightforward approach (and the one we will adopt) would be to set  $\Lambda = G_{a\gamma\gamma'}^{-1}$  and use  $G_{a\gamma\gamma'}^{-1}$  as the cut-off scale, although it is not mandatory.

In this case, the photon propagator should be modified. If we keep all possible interactions and corrections to  $\mathcal{O}(G_{a\gamma\gamma'}^2)$ , the quadratic lagrangian for the photon is given by

$$\mathcal{L}_{\text{kin}} = -\frac{1}{4} F_{\mu\nu} F^{\mu\nu} + \frac{cG_{a\gamma\gamma'}^2}{4} \partial_\rho F_{\mu\nu} \partial^\rho F^{\mu\nu} - \frac{1}{2\xi} [(\partial_\mu A^\mu)^2 - cG_{a\gamma\gamma'}^2 (\partial_\rho \partial_\mu A^\mu)^2] \quad (\text{A4})$$

in the  $\xi$ -gauge. This can be rewritten as

$$\frac{1}{2} A_\mu \left[ \partial^2 g^{\mu\nu} - (1 - \frac{1}{\xi} \partial^\mu \partial^\nu) \right] [1 + cG_{a\gamma\gamma'}^2] A_\nu, \quad (\text{A5})$$

up to total divergences. The photon propagator is written as

$$\frac{-i}{(k^2 + i\epsilon)[1 - cG_{a\gamma\gamma'}^2 k^2]} [g_{\mu\nu} + (1 - \xi)k]. \quad (\text{A6})$$

Note that the propagating part of the propagator can be rewritten as

$$\frac{1}{k^2[1 - cG_{a\gamma\gamma'}^2 k^2]} = \frac{1}{k^2} - \frac{1}{k^2 - \frac{1}{cG_{a\gamma\gamma'}^2}} \quad (\text{A7})$$

from which we see that the quartic derivative of the photon field plays the role of the Pauli-Villars regulator, which introduces a ‘ghost’ with a mass term  $(cG_{a\gamma\gamma'}^2)^{-1}$ . In order to prevent the super-luminal propagation of the ghost, we require  $c > 0$ .

It is interesting to note that the non-renormalizable term of Eq. (A3) has parallels with the Lee-Wick Standard Model. In this model, by putting the Pauli-Villars regulator as Eq. (A7), the degree of divergence in the loop diagram is reduced. As a result, QED becomes UV finite [66, 67], and when extended to the SM, the quadratic divergence in the Higgs mass correction is removed [68]. In order to make the theory unitary, the integration contour in the Feynman diagram is modified, at the price of which the causality is violated microscopically [69–71].

With the inclusion of the additional counter term, we can write the renormalized form of  $\Pi(q^2)$ ,

$$\Pi_R(q^2) = \Pi(q^2) - \Pi(0) - q^2 \Pi'(0) \quad (\text{A8})$$

where  $\Pi_R(q^2)$  is finite, and  $\Pi'(0) = \frac{d\Pi(q^2)}{dq^2} \Big|_{q^2=0}$ .

The expression for  $\Pi_R(q^2)$  can be found in Eq. (12), as well as its application in calculating electron and muon  $g - 2$ .

---

[1] G. Aad *et al.* [ATLAS Collaboration], Phys. Lett. B **716**, 1 (2012) doi:10.1016/j.physletb.2012.08.020 [arXiv:1207.7214 [hep-ex]].

[2] S. Chatrchyan *et al.* [CMS Collaboration], Phys. Lett. B **716**, 30 (2012) doi:10.1016/j.physletb.2012.08.021 [arXiv:1207.7235 [hep-ex]].

[3] C. Patrignani *et al.* [Particle Data Group], Chin. Phys. C **40**, no. 10, 100001 (2016). doi:10.1088/1674-1137/40/10/100001

[4] L. J. Hall, K. Jedamzik, J. March-Russell and S. M. West, JHEP **1003**, 080 (2010) doi:10.1007/JHEP03(2010)080 [arXiv:0911.1120 [hep-ph]].

[5] R. Essig *et al.*, arXiv:1311.0029 [hep-ph].

[6] J. Alexander *et al.*, arXiv:1608.08632 [hep-ph].

[7] N. Arkani-Hamed, D. P. Finkbeiner, T. R. Slatyer and N. Weiner, Phys. Rev. D **79**, 015014 (2009) doi:10.1103/PhysRevD.79.015014 [arXiv:0810.0713 [hep-ph]].

[8] Y. Nomura and J. Thaler, Phys. Rev. D **79**, 075008 (2009) doi:10.1103/PhysRevD.79.075008 [arXiv:0810.5397 [hep-ph]].

[9] B. Holdom, Phys. Lett. **166B**, 196 (1986). doi:10.1016/0370-2693(86)91377-8

[10] H. Davoudiasl, H. S. Lee and W. J. Marciano, Phys. Rev. D **85**, 115019 (2012) doi:10.1103/PhysRevD.85.115019 [arXiv:1203.2947 [hep-ph]].

[11] H. Davoudiasl, H. S. Lee and W. J. Marciano, Phys. Rev. Lett. **109**, 031802 (2012) doi:10.1103/PhysRevLett.109.031802 [arXiv:1205.2709 [hep-ph]].

[12] H. S. Lee and M. Sher, Phys. Rev. D **87**, no. 11, 115009 (2013) doi:10.1103/PhysRevD.87.115009 [arXiv:1303.6653 [hep-ph]].

[13] H. Davoudiasl, H. S. Lee, I. Lewis and W. J. Marciano, Phys. Rev. D **88**, no. 1, 015022 (2013) doi:10.1103/PhysRevD.88.015022 [arXiv:1304.4935 [hep-ph]].

ph]].

[14] K. Kong, H. S. Lee and M. Park, Phys. Rev. D **89**, no. 7, 074007 (2014) doi:10.1103/PhysRevD.89.074007 [arXiv:1401.5020 [hep-ph]].

[15] H. Davoudiasl, H. S. Lee and W. J. Marciano, Phys. Rev. D **89**, no. 9, 095006 (2014) doi:10.1103/PhysRevD.89.095006 [arXiv:1402.3620 [hep-ph]].

[16] D. Kim, H. S. Lee and M. Park, JHEP **1503**, 134 (2015) doi:10.1007/JHEP03(2015)134 [arXiv:1411.0668 [hep-ph]].

[17] H. Davoudiasl, H. S. Lee and W. J. Marciano, Phys. Rev. D **92**, no. 5, 055005 (2015) doi:10.1103/PhysRevD.92.055005 [arXiv:1507.00352 [hep-ph]].

[18] K. Kaneta, H. S. Lee and S. Yun, Phys. Rev. Lett. **118**, no. 10, 101802 (2017) doi:10.1103/PhysRevLett.118.101802 [arXiv:1611.01466 [hep-ph]].

[19] K. Choi, H. Kim and T. Sekiguchi, Phys. Rev. D **95**, no. 7, 075008 (2017) doi:10.1103/PhysRevD.95.075008 [arXiv:1611.08569 [hep-ph]].

[20] K. Kaneta, H. S. Lee and S. Yun, Phys. Rev. D **95**, no. 11, 115032 (2017) doi:10.1103/PhysRevD.95.115032 [arXiv:1704.07542 [hep-ph]].

[21] P. Agrawal, G. Marques-Tavares and W. Xue, JHEP **1803**, 049 (2018) doi:10.1007/JHEP03(2018)049 [arXiv:1708.05008 [hep-ph]].

[22] N. Kitajima, T. Sekiguchi and F. Takahashi, Phys. Lett. B **781**, 684 (2018) doi:10.1016/j.physletb.2018.04.024 [arXiv:1711.06590 [hep-ph]].

[23] K. Choi, H. Kim and T. Sekiguchi, arXiv:1802.07269 [hep-ph].

[24] J. E. Kim, Phys. Rev. Lett. **43**, 103 (1979). doi:10.1103/PhysRevLett.43.103

[25] M. A. Shifman, A. I. Vainshtein and V. I. Zakharov, Nucl. Phys. B **166**, 493 (1980). doi:10.1016/0550-3213(80)90209-6

[26] H. S. Lee and M. S. Seo, Phys. Lett. B **767**, 69 (2017) doi:10.1016/j.physletb.2017.01.058 [arXiv:1608.02708 [hep-ph]].

[27] J. Jaeckel, Frascati Phys. Ser. **56**, 172 (2012) [arXiv:1303.1821 [hep-ph]].

[28] B. Aubert *et al.* [BaBar Collaboration], Nucl. Instrum. Meth. A **479**, 1 (2002) doi:10.1016/S0168-9002(01)02012-5 [hep-ex/0105044].

[29] J. P. Lees *et al.* [BaBar Collaboration], Nucl. Instrum. Meth. A **726**, 203 (2013) doi:10.1016/j.nima.2013.04.029 [arXiv:1301.2703 [hep-ex]].

[30] V. Shtabovenko, R. Mertig and F. Orellana, Comput. Phys. Commun. **207**, 432 (2016) doi:10.1016/j.cpc.2016.06.008 [arXiv:1601.01167 [hep-ph]].

[31] R. Mertig, M. Bohm and A. Denner, Comput. Phys. Commun. **64**, 345 (1991). doi:10.1016/0010-4655(91)90130-D

[32] R. Essig, J. Mardon, M. Papucci, T. Volansky and Y. M. Zhong, JHEP **1311**, 167 (2013) doi:10.1007/JHEP11(2013)167 [arXiv:1309.5084 [hep-ph]].

[33] B. Aubert *et al.* [BaBar Collaboration], arXiv:0808.0017 [hep-ex].

[34] J. P. Lees *et al.* [BaBar Collaboration], Phys. Rev. Lett. **119**, no. 13, 131804 (2017) doi:10.1103/PhysRevLett.119.131804 [arXiv:1702.03327 [hep-ex]].

[35] A. Pukhov *et al.*, hep-ph/9908288.

[36] A. Belyaev, N. D. Christensen and A. Pukhov, Comput. Phys. Commun. **184**, 1729 (2013) doi:10.1016/j.cpc.2013.01.014 [arXiv:1207.6082 [hep-ph]].

[37] T. Skwarnicki, DESY-F31-86-02, DESY-F-31-86-02.

[38] J. P. Lees *et al.* [BaBar Collaboration], Phys. Rev. Lett. **113**, no. 20, 201801 (2014) doi:10.1103/PhysRevLett.113.201801 [arXiv:1406.2980 [hep-ex]].

[39] T. Abe *et al.* [Belle-II Collaboration], arXiv:1011.0352 [physics.ins-det].

[40] C. Hearty, *Dark sector searches at B-factories and outlook for Belle II*, <https://indico.fnal.gov/getFile.py/access?contribId=123&sessionId=9&resId=0&materialId=slides&confId=13702>.

[41] F. Jegerlehner and A. Nyffeler, Phys. Rept. **477**, 1 (2009) doi:10.1016/j.physrep.2009.04.003 [arXiv:0902.3360 [hep-ph]].

[42] M. Lindner, M. Platscher and F. S. Queiroz, Phys. Rept. **731**, 1 (2018) doi:10.1016/j.physrep.2017.12.001 [arXiv:1610.06587 [hep-ph]].

[43] P. J. Mohr, B. N. Taylor and D. B. Newell, Rev. Mod. Phys. **84**, 1527 (2012) doi:10.1103/RevModPhys.84.1527 [arXiv:1203.5425 [physics.atom-ph]].

[44] G. W. Bennett *et al.* [Muon g-2 Collaboration], Phys. Rev. Lett. **89**, 101804 (2002) Erratum: [Phys. Rev. Lett. **89**, 129903 (2002)] doi:10.1103/PhysRevLett.89.129903, 10.1103/PhysRevLett.89.101804 [hep-ex/0208001].

[45] G. W. Bennett *et al.* [Muon g-2 Collaboration], Phys. Rev. Lett. **92**, 161802 (2004) doi:10.1103/PhysRevLett.92.161802 [hep-ex/0401008].

[46] G. W. Bennett *et al.* [Muon g-2 Collaboration], Phys. Rev. D **73**, 072003 (2006) doi:10.1103/PhysRevD.73.072003 [hep-ex/0602035].

[47] J. Grange *et al.* [Muon g-2 Collaboration], arXiv:1501.06858 [physics.ins-det].

[48] R. Bouchendira, P. Clade, S. Guellati-Khelifa, F. Nez and F. Biraben, Phys. Rev. Lett. **106**, 080801 (2011) doi:10.1103/PhysRevLett.106.080801 [arXiv:1012.3627 [physics.atom-ph]].

[49] D. Hanneke, S. Fogwell and G. Gabrielse, Phys. Rev. Lett. **100**, 120801 (2008) doi:10.1103/PhysRevLett.100.120801 [arXiv:0801.1134 [physics.atom-ph]].

[50] D. Hanneke, S. F. Hoogerheide and G. Gabrielse, Phys. Rev. A **83**, 052122 (2011) doi:10.1103/PhysRevA.83.052122 [arXiv:1009.4831 [physics.atom-ph]].

[51] T. Aoyama, M. Hayakawa, T. Kinoshita and M. Nio, Phys. Rev. Lett. **109**, 111807 (2012) doi:10.1103/PhysRevLett.109.111807 [arXiv:1205.5368 [hep-ph]].

[52] M. Endo, K. Hamaguchi and G. Mishima, Phys. Rev. D **86**, 095029 (2012) doi:10.1103/PhysRevD.86.095029 [arXiv:1209.2558 [hep-ph]].

[53] W. J. Marciano, A. Masiero, P. Paradisi and M. Passera, Phys. Rev. D **94**, no. 11, 115033 (2016) doi:10.1103/PhysRevD.94.115033 [arXiv:1607.01022 [hep-ph]].

[54] M. S. Atiya *et al.*, Phys. Rev. Lett. **69**, 733 (1992). doi:10.1103/PhysRevLett.69.733

[55] A. V. Artamonov *et al.* [E949 Collaboration], Phys. Rev. Lett. **101**, 191802 (2008) doi:10.1103/PhysRevLett.101.191802 [arXiv:0808.2459 [hep-ex]].

A. V. Artamonov *et al.* [BNL-E949 Collaboration], Phys. Rev. D **79**, 092004 (2009) doi:10.1103/PhysRevD.79.092004 [arXiv:0903.0030 [hep-ex]].

[56] M. N. Achasov *et al.*, Eur. Phys. J. C **12**, 25 (2000). doi:10.1007/s100529900222

[57] M. Anelli *et al.* [SHiP Collaboration], arXiv:1504.04956 [physics.ins-det].

[58] B. Batell, M. Pospelov and A. Ritz, Phys. Rev. D **80**, 095024 (2009) doi:10.1103/PhysRevD.80.095024 [arXiv:0906.5614 [hep-ph]].

[59] P. deNiverville, C. Y. Chen, M. Pospelov and A. Ritz, Phys. Rev. D **95**, no. 3, 035006 (2017) doi:10.1103/PhysRevD.95.035006 [arXiv:1609.01770 [hep-ph]].

[60] A. A. Aguilar-Arevalo *et al.* [MiniBooNE Collaboration], Phys. Rev. Lett. **118**, no. 22, 221803 (2017) doi:10.1103/PhysRevLett.118.221803 [arXiv:1702.02688 [hep-ex]].

[61] Y. J. Ko *et al.*, Phys. Rev. Lett. **118**, no. 12, 121802 (2017) doi:10.1103/PhysRevLett.118.121802 [arXiv:1610.05134 [hep-ex]].

[62] H. Park, Phys. Rev. Lett. **119**, no. 8, 081801 (2017) doi:10.1103/PhysRevLett.119.081801 [arXiv:1705.02470 [hep-ph]].

[63] D. Banerjee *et al.* [NA64 Collaboration], Phys. Rev. D **97**, no. 7, 072002 (2018) doi:10.1103/PhysRevD.97.072002 [arXiv:1710.00971 [hep-ex]].

[64] H. K. Dreiner, J. F. Fortin, C. Hanhart and L. Ubaldi, Phys. Rev. D **89**, no. 10, 105015 (2014) doi:10.1103/PhysRevD.89.105015 [arXiv:1310.3826 [hep-ph]].

[65] J. Redondo and G. Raffelt, JCAP **1308**, 034 (2013) doi:10.1088/1475-7516/2013/08/034 [arXiv:1305.2920 [hep-ph]].

[66] T. D. Lee and G. C. Wick, Nucl. Phys. B **9**, 209 (1969). doi:10.1016/0550-3213(69)90098-4

[67] T. D. Lee and G. C. Wick, Phys. Rev. D **2**, 1033 (1970). doi:10.1103/PhysRevD.2.1033

[68] B. Grinstein, D. O’Connell and M. B. Wise, Phys. Rev. D **77**, 025012 (2008) doi:10.1103/PhysRevD.77.025012 [arXiv:0704.1845 [hep-ph]].

[69] R. E. Cutkosky, P. V. Landshoff, D. I. Olive and J. C. Polkinghorne, Nucl. Phys. B **12**, 281 (1969). doi:10.1016/0550-3213(69)90169-2

[70] T. D. Lee and G. C. Wick, Phys. Rev. D **3**, 1046 (1971). doi:10.1103/PhysRevD.3.1046

[71] S. Coleman, “Acausality”, in Erice 1969, Ettore Majorana School On Subnuclear Phenomena, New York, 282 (1970).